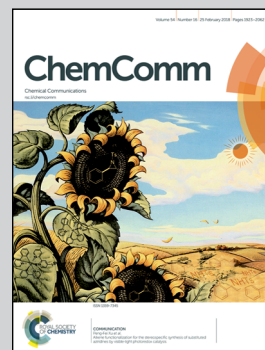


**Showcasing research from the Laboratory of Organic Electronics,  
Linköping University, Sweden**

Organic semiconductor perylenetetracarboxylic diimide (PTCDI) electrodes for electrocatalytic reduction of oxygen to hydrogen peroxide

The commercial organic pigment perylene bisimide is a stable n-type electrocatalyst for oxygen reduction to  $\text{H}_2\text{O}_2$  in a wide range of aqueous conditions, demonstrating a promising route for more sustainable industrial production of peroxide. Our finding that an intrinsic (undoped) molecular semiconductor can support high catalytic electron currents opens new avenues for using cheap organic pigments in catalysis.

**As featured in:**



See Eric Daniel Głowacki et al.,  
*Chem. Commun.*, 2018, **54**, 1960.

Cite this: *Chem. Commun.*, 2018, 54, 1960Received 3rd November 2017,  
Accepted 18th December 2017

DOI: 10.1039/c7cc08471d

rsc.li/chemcomm

# Organic semiconductor perylenetetracarboxylic diimide (PTCDI) electrodes for electrocatalytic reduction of oxygen to hydrogen peroxide†

Magdalena Warczak,<sup>a</sup> Maciej Gryszel,<sup>a</sup> Marie Jakešová,<sup>a</sup> Vedran Đerek<sup>ab</sup> and Eric Daniel Głowacki<sup>id</sup> <sup>★a</sup>

Hydrogen peroxide is one of the most important industrial chemicals and there is great demand for the production of H<sub>2</sub>O<sub>2</sub> using more sustainable and environmentally benign methods. We show electrochemical production of H<sub>2</sub>O<sub>2</sub> by the reduction of O<sub>2</sub>, enabled by an organic semiconductor catalyst, *N,N'*-dimethyl perylenetetracarboxylic diimide (PTCDI). We make PTCDI cathodes that are capable of stable and reusable operation in aqueous electrolytes in a pH range of 1–13 with a catalytic figure of merit as high as 26 kg H<sub>2</sub>O<sub>2</sub> per g catalyst per h. These performance and stability open new avenues for organic small molecule semiconductors as electrocatalysts.

Hydrogen peroxide is a remarkably versatile molecule for chemical industry, materials processing, agriculture, and medical applications.<sup>1</sup> Its increasing use as a “green” oxidant has generated great interest in finding more environmentally friendly and less energetically demanding alternatives to the incumbent anthraquinone oxidation (AO) process.<sup>2,3</sup> The AO process involves high-pressure hydrogenation on noble metal catalysts of alkylanthraquinones in organic solvents, followed by aqueous extraction to recover the H<sub>2</sub>O<sub>2</sub>. The need for H<sub>2</sub> of fossil fuel origin, and for large volumes of organic solvents, accounts for a substantial environmental footprint of H<sub>2</sub>O<sub>2</sub>. Direct electrochemical reduction of O<sub>2</sub> to H<sub>2</sub>O<sub>2</sub> has been proposed as an alternative.<sup>2</sup> However, the list of materials suitable for selective electrocatalysis of oxygen reduction to peroxide is very limited. Electrosynthesis of peroxide in highly alkaline solutions on carbon cathodes is employed industrially on a limited scale;<sup>4</sup> however, it has not been found to be competitive under neutral to acidic conditions.<sup>5</sup> Recently, some coordination compounds of iron and cobalt have been shown to reduce oxygen to peroxide under acidic conditions.<sup>6,7</sup> The starting point for this work

is the search for a simple, low-cost, scalable, and stable high performance electrocatalyst for H<sub>2</sub>O<sub>2</sub> production, ideally under various pH conditions. Since metallic electrodes, as well as many metal salts, catalyze<sup>8,9</sup> the further reduction of H<sub>2</sub>O<sub>2</sub> to H<sub>2</sub>O, or peroxide disproportionation to H<sub>2</sub>O and O<sub>2</sub>, organic conducting materials could be a logical choice for selective electrochemical H<sub>2</sub>O<sub>2</sub> production. Organic semiconductors have made great impact in the field of light-emitting diode technology, and are emerging materials in energy harvesting and thin-film electronics applications. Much less attention has been given to their use in electrocatalytic applications primarily due to the fact that many organic semiconductors degrade rapidly under aqueous and oxygenated conditions. Herein we report that PTCDI belongs to a class of molecular materials which challenges this point of view. The possibility of oxygen reduction reactions (ORR) has recently been elaborated by several research groups. Poly(3-hexylthiophene) has been reported to act as a photocathodic catalyst in one-electron reduction of oxygen to give superoxide radicals.<sup>10,11</sup> Conducting polymer poly(3,4-ethylenedioxythiophene) electrodes have also been demonstrated to support the oxygen reduction reaction under cathodic polarization.<sup>12</sup> However, polythiophenes suffer from limited stability, and are known to oxidize and degrade under aqueous conditions.<sup>13</sup> In our recent work, we have shown that carbonyl pigments, such as acridones, are photocathodic materials that selectively give two-electron photoreduction of O<sub>2</sub> to hydrogen peroxide, and have photocathodic activity and excellent stability in the pH range of 1–12.<sup>14,15</sup> This work encouraged us to explore other organic pigments with similar carbonyl functionality but different energy levels. The acridones have high-lying, and thus strongly-reducing, conduction band levels (around −2.9 eV *versus* vacuum, or −1.6 V *vs.* NHE), combined with facile p-type transport, therefore photocathodic behavior is observed. Injection of electrons from a metallic electrode into these materials, however, is impossible. Herein we evaluate perylenetetracarboxylic diimides (PTCDI), which have, in contrast, a lower-lying conduction band. This electronic structure affords the possibility of electron injection and stable n-type transport, so one can hypothesize cathodic electrocatalytic

<sup>a</sup> Laboratory of Organic Electronics, ITN Campus Norrköping, Linköpings Universitet, Bredgatan 34, 60221, Norrköping, Sweden. E-mail: eric.glowacki@liu.se

<sup>b</sup> Center of Excellence for Advanced Materials and Sensing Devices, Ruđer Bošković Institute, 10000 Zagreb, Croatia

† Electronic supplementary information (ESI) available: SEM and reflectance of PTCDI electrodes, frontier energy level calculations, and PTCDI electrochemistry in oxygen-free water. See DOI: 10.1039/c7cc08471d



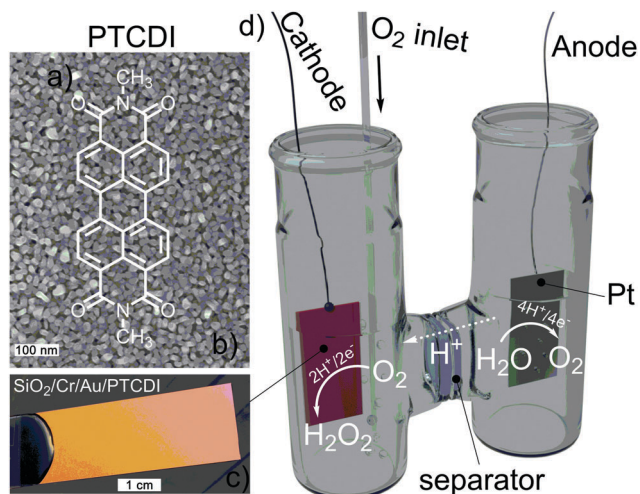


**Fig. 1** (a) The molecular structure of PTCDI, which functions as an n-type conducting electrocatalyst. (b) Scanning electron micrograph of a 100 nm-thick film of PTCDI evaporated on a Cr/Au thin film substrate, showing the distinctive nanocrystalline grain morphology formed by PTCDI. (c) 2 × 5 cm SiO<sub>2</sub>/Cr/Au/PTCDI cathode used in electrolyzer experiments. (d) Oxygen-to-peroxide electrolyzer configuration used throughout this work. The PTCDI semiconductor cathode operates in an O<sub>2</sub>-saturated solution, which is separated from the anode chamber by a glass frit or an agarose bridge. The oxygen evolution reaction occurs on the platinum anode.

applications. PTCDis are commercial organic pigments used in inks, outdoor paints, and cosmetics.<sup>16,17</sup> They are remarkable for their low cost and stability, and the range of pigmentary properties that can be achieved *via* crystal engineering.<sup>18</sup> Their properties as organic semiconductors have been exploited in organic photovoltaics,<sup>19,20</sup> photodiodes,<sup>21,22</sup> and thin-film transistor applications,<sup>23</sup> where they are known to have electron mobility up to 1 cm<sup>2</sup> V<sup>-1</sup> s<sup>-1</sup> for the archetypal *N,N'*-dimethyl perylenetetracarboxylic diimide used in this work (Fig. 1a).

We fabricated semiconductor electrodes for electrocatalytic oxygen reduction using a metallic thin film covered with a layer of the semiconducting small molecule PTCDI (Fig. 1a), which was sublimed under high vacuum to produce a nanocrystalline morphology (Fig. 1b and c; ESI,† Fig. S1). Scanning electron micrographs reveal continuous layers of rounded crystallites of average diameter 57 ± 7 nm when evaporated on Au. Various metallic films were evaluated as back electrodes, such as titanium, indium tin oxide, fluorine-doped tin oxide, and finally gold. Mechanical delamination of the PTCDI layer was found to occur in all cases, except Cr/Au, where adhesion of PTCDI was ideal. It became immediately apparent that 50 nm gold films on top of a 2 nm chromium sticking layer afforded a combination of high currents and excellent stability, and were thus used throughout this study as a back contact material. 100 nm-thick PTCDI films were used throughout, as we found no strong dependence of the cathodic current on the thickness (ESI,† Fig. S2). We estimated *via* cyclic voltammetry in a nonaqueous electrolyte the valence and conduction band levels of the PTCDI (ESI,† Fig. S3), calculating  $E_{CB}$  of -3.9 eV *versus* vacuum, or -0.6 V *vs.* NHE, which are amply reductive with respect to the standard potential for O<sub>2</sub> reduction to H<sub>2</sub>O<sub>2</sub>, +0.7 V. The PTCDI electrodes were then characterized under

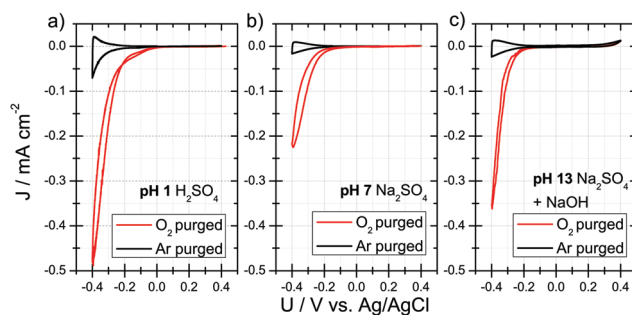


**Fig. 2** Cyclic voltammetry of Au/PTCDI electrodes at pH 1 (a), pH 7 (b) and pH 13 (c) under oxygenated and deoxygenated (Ar) conditions using Ag/AgCl (3 M KCl) reference electrodes. Characteristic ORR behavior is visible in all cases. The cathodic current under argon purging is attributed to proton reduction to H<sub>2</sub>.

aqueous conditions using cyclic voltammetry and galvanostatic electrolysis experiments with separated cathode and anode chambers, as shown in Fig. 1d. Cathodic currents are visible with an onset around 0 V *vs.* Ag/AgCl at pH 1, while at higher pH 7–13 the onset shifts to -0.15 V (Fig. 2a–c). Purging the cathode chamber with argon leads to a substantial decrease of these cathodic currents, while saturation with oxygen enhances them, unequivocally implicating ORR (Fig. 2). The remaining cathodic current under argon purged conditions is attributed to the hydrogen evolution reaction (HER). Further cathodic polarization beyond -0.4 V leads to dominance of HER, where current densities as high as 6 mA cm<sup>-2</sup> can be achieved; however, this is beyond the scope of the present work (ESI,† Fig. S4). Using the horseradish peroxidase/tetramethylbenzidine assay,<sup>14</sup> we determined that galvanostatic cathodic electrolysis with O<sub>2</sub>-bubbled electrolytes gives H<sub>2</sub>O<sub>2</sub> as the dominant product of oxygen reduction. We found that H<sub>2</sub>O<sub>2</sub> production occurs over the entire pH range, with higher Faraday efficiency for the 2e<sup>-</sup>/2H<sup>+</sup> acidic process. At pH 1, we observed the two-regime Tafel slope characteristic of ORR, with 98 and 82 mV dec<sup>-1</sup>, and an exchange current density of 1 μA cm<sup>-2</sup>.

Having established peroxide as the product of ORR, we focused on the deployment of PTCDI electrodes for practical electrosynthesis of H<sub>2</sub>O<sub>2</sub>. Galvanostatic measurements were conducted with the cathode and anode chambers separated by an agarose bridge, with a constant flow of oxygen into the catholyte (150 mL min<sup>-1</sup>). The concentration of H<sub>2</sub>O<sub>2</sub> and the corresponding Faraday efficiency over time of electrolysis at different pH and current density values are shown in Fig. 3a and b. H<sub>2</sub>O<sub>2</sub> was accumulated in the catholyte, with the Faraday efficiency, generation rate, and total concentration highest at low pH. Na<sub>2</sub>SO<sub>4</sub>, with H<sub>2</sub>SO<sub>4</sub> and NaOH added to adjust pH, was used in all cases to provide a stable electrolyte without undesired side reactions. In particular, chloride containing electrolytes were avoided to prevent problems with chloride oxidation and also etching of the gold layers. The most optimal conditions found for H<sub>2</sub>O<sub>2</sub> generation were pH 1 and 0.5 mA cm<sup>-2</sup> (Fig. 3c). Under these conditions a stable cell voltage of -2.5 V was maintained for 48 hours, with the agarose separator being the limiting factor for obtaining lower voltages. Under all conditions of





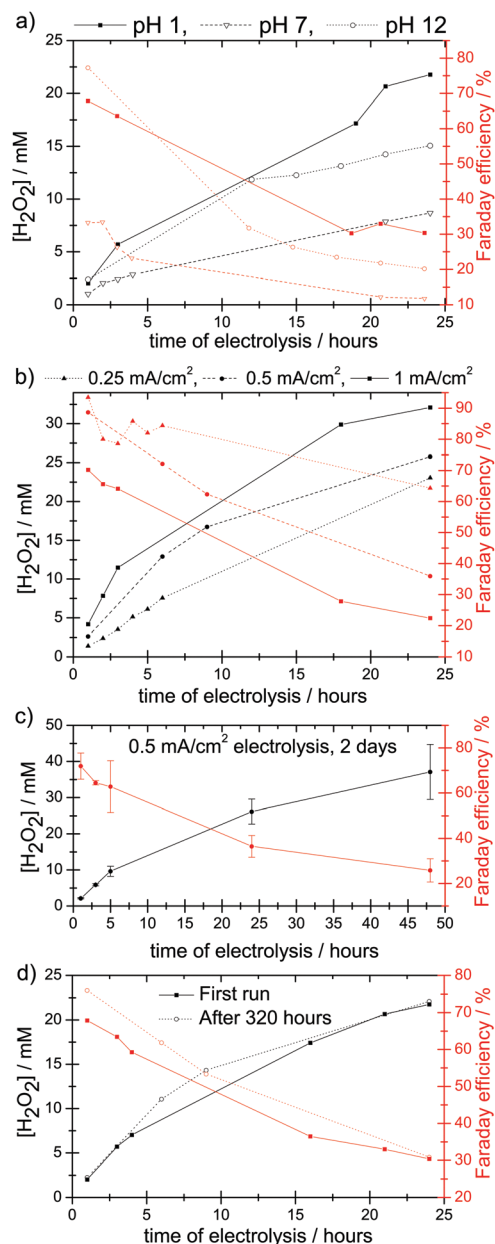


Fig. 3 (a) Galvanostatic oxygen-to-peroxide electrolysis using a current density of  $0.5 \text{ mA cm}^{-2}$  at pH 1, 7, and 12, showing the results for catholyte  $H_2O_2$  concentration and the corresponding Faraday efficiency. (b) Galvanostatic electrolysis results in pH 1 electrolyte for  $0.25$ ,  $0.5$ , and  $1 \text{ mA cm}^{-2}$ .  $0.5 \text{ mA cm}^{-2}$  gives the best trade-off of the generation rate and efficiency. (c) Statistics for pH 1 electrolysis with different cathodes with  $0.5 \text{ mA cm}^{-2}$ ,  $n = 4$ . Cell voltage remained constant at  $-2.5 \text{ V}$ . (d) A total of 344 h of electrolysis under pH 1 conditions on a single sample: first scan and last scan starting at hour 320.

different current densities and pH values, the Faraday efficiency decreased over time. Two explanations for this observation are possible: either the electrocatalyst suffers from degradation or the increased  $H_2O_2$  concentration begins to favor the subsequent reduction of peroxide to water. We establish that the second hypothesis is correct, as the same cathode was reused for up to six rounds of electrolysis, with the Faraday efficiency value returning to the initial higher values at the beginning of the electrolysis

experiment (Fig. 3d). In total, samples were used for up to 344 hours in this study without degradation in performance. SEM imaging and optical reflectivity measurements of electrodes before and after extended electrolysis revealed no apparent morphological changes or changes in optical absorbance, respectively (ESI,† Fig. S1 and S5). Secondly, the further reduction of  $H_2O_2$  to  $H_2O$  can be clearly evidenced by measuring the cathodic current upon the addition of peroxide to the electrolyte (ESI,† Fig. S4). Therefore the problem of why higher equilibrium  $H_2O_2$  concentrations are not possible is because once  $[H_2O_2]$  reaches similar values as  $[O_2]$  ( $\approx 1 \text{ mM}$  under 1 atm of pure  $O_2$ ), the further reduction of  $H_2O_2$  to  $H_2O$  becomes competitive with ORR. Future electrocatalyst improvement should focus on obtaining molecular semiconductors with higher overpotential for  $H_2O_2$  reduction. Overall, the performance benchmarks of PTCDI cathodes for hydrogen peroxide production are competitive, with best results at initial rates for pH 1: 26 kg  $H_2O_2$  are produced per one gram of catalyst per hour. Considering the initial rates, this process consumes 4.8 kW h per kg of  $H_2O_2$ , corresponding to a 21% thermodynamic electrical energy-to-peroxide conversion efficiency. Higher peroxide yields and an eventual industrial application could be enabled by incorporating PTCDI electrodes into flow reactors, as has been suggested before for upscaled peroxide production.<sup>4</sup>

Organic molecular semiconductors comprise a rich field of applied research; however, deployment of organic semiconductors as electrocatalysts represents an untapped direction. Herein we have shown that the archetypical carbonyl pigment semiconductor PTCDI can be a stable n-type electrocatalyst which can facilitate the oxygen reduction reaction to produce  $H_2O_2$ . Our finding that an intrinsic (undoped) molecular semiconductor can support such high catalytic electron currents is an unexpected result which should stimulate research into deploying such materials as electrocatalysts. On the other hand, our results make electrosynthesis of  $H_2O_2$  closer to being an approach competitive with the incumbent AO process of production for this key industrial chemical. Future research should focus on molecular structures which suppress the reduction of  $H_2O_2$  to  $H_2O$  and on exploring other possibilities of organic semiconductors as catalytic materials in general.

We acknowledge funding from the Wallenberg Center for Molecular Medicine at Linköping University for support of this work.

## Conflicts of interest

There are no conflicts to declare.

## Notes and references

- 1 G. Goor, J. Glenneberg and S. Jacobi, Hydrogen Peroxide, *Ullmann's Encyclopedia of Industrial Chemistry*, 2012, vol. 18, pp. 393–427.
- 2 J. M. Campos-Martin, G. Blanco-Brieva and J. L. G. Fierro, *Angew. Chem., Int. Ed.*, 2006, **45**, 6962–6984.
- 3 A. Goti and F. Cardona, in *Green Chemical Reactions*, ed. P. Tundo and V. Esposito, Springer, 2008, pp. 191–212.
- 4 C. Oloman and A. P. Watkinson, *J. Appl. Electrochem.*, 1979, **9**, 117–123.
- 5 Z. Qiang, J. Chang and C. Huang, *Water Res.*, 2002, **36**, 85–94.
- 6 Y. Yamada, S. Yoshida, T. Honda and S. Fukuzumi, *Energy Environ. Sci.*, 2011, **4**, 2822–2825.



- 7 K. Mase, M. Yoneda, Y. Yamada and S. Fukuzumi, *ACS Energy*, 2016, **1**, 913–919.
- 8 C. Song and J. Zhang, in *PEM Fuel Cell Electrocatalysts and Catalyst Layers: Fundamentals and Applications*, ed. J. Zhang, Springer, London, 2008, pp. 89–134.
- 9 L. Dai, Y. Xue, L. Qu, H.-J. Choi and J.-B. Baek, *Chem. Rev.*, 2015, **115**, 4823–4892.
- 10 G. Suppes, E. Ballard and S. Holdcroft, *Polym. Chem.*, 2013, **4**, 5345–5350.
- 11 S. Bellani, A. Ghadirzadeh, L. Meda, A. Savoini, A. Tacca, G. Marra, R. Meira, J. Morgado, F. Di Fonzo and M. R. Antognazza, *Adv. Funct. Mater.*, 2015, **25**, 4531–4538.
- 12 E. Mitraka, M. J. Jafari, M. Vagin, X. Liu, M. Fahlman, T. Ederth, M. Berggren, M. P. Jonsson and X. Crispin, *J. Mater. Chem. A*, 2017, **5**, 4404–4412.
- 13 A. Elschner, S. Kirchmeyer, W. Lovenich, U. Merker and K. Reuter, *PEDOT: Principles and Applications of an Intrinsically Conductive Polymer*, CRC Press, 2011.
- 14 M. Jakešová, D. H. Apaydin, M. Sytnyk, K. Oppelt, W. Heiss, N. S. Sariciftci and E. D. Głowacki, *Adv. Funct. Mater.*, 2016, **26**, 5248–5254.
- 15 M. K. Węclawski, M. Jakešová, M. Charyton, N. Demitri, B. Koszarna, K. Oppelt, S. Sariciftci, D. T. Gryko and E. D. Głowacki, *J. Mater. Chem. A*, 2017, **5**, 20780–20788.
- 16 H. Zollinger, *Color Chemistry. Syntheses, Properties and Applications of Organic Dyes and Pigments*, Wiley-VCH, Weinheim, 3rd edn, 2003.
- 17 *High Performance Pigments*, ed. E. B. Faulkner and R. J. Schwartz, Wiley-VCH, Weinheim, 2nd edn, 2009.
- 18 G. Klebe, F. Graser, E. Hädicke and J. Berndt, *Acta Crystallogr., Sect. B: Struct. Sci.*, 1989, **45**, 69–77.
- 19 C. W. Tang, *Appl. Phys. Lett.*, 1986, **48**, 183–185.
- 20 X. Zhan, A. Facchetti, S. Barlow, T. J. Marks, M. A. Ratner, M. R. Wasielewski and S. R. Marder, *Adv. Mater.*, 2011, **23**, 268–284.
- 21 T. Someya, Y. Kato, S. Iba, Y. Noguchi, T. Sekitani, H. Kawaguchi and T. Sakurai, *IEEE Trans. Electron Devices*, 2005, **52**, 2502–2511.
- 22 M. Bednorz, G. J. Matt, E. D. Głowacki, T. Fromherz, C. J. Brabec, M. C. Scharber, H. Sitter and N. S. Sariciftci, *Org. Electron.*, 2013, **14**, 1344–1350.
- 23 M. Gsänger, D. Bialas, L. Huang, M. Stolte and F. Würthner, *Adv. Mater.*, 2016, **28**, 3615–3645.

